Optics and Lasers in Engineering 177 (2024) 108125

Contents lists available at ScienceDirect

Optics and Lasers in Engineering

journal homepage: www.elsevier.com/locate/optlaseng

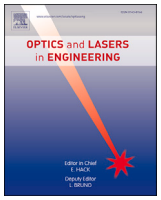

Tracking hydrodynamic disturbances with fibre-optic whiskers

Raphael Glick [a,*], Christoph Brücker [a], Matthias Fabian [b], Kenneth T.V. Grattan [b]

[a] Aeronautics and Aerospace Research Centre, School of Science and Technology, City University of London, London, EC1V 0HB, United Kingdom
[b] Research Centre for Photonics and Instrumentation, School of Science and Technology, City University of London, London, EC1V 0HB, United Kingdom

ARTICLE INFO

Keywords:
Fibre Bragg gratings
Optical fibres
Sensors
Artificial whiskers
Bio-mimicry
Hydrodynamic tracking
Source localisation

ABSTRACT

Previous research has identified the capabilities of artificial whisker sensor arrays as an innovative method of tracking and evaluating flow events and disturbances. In this work, a new approach is put forward, focusing on achieving enhanced sensitivity and improved performance of fibre-optic whisker sensors, based on the principle of fibre Bragg Grating (FBG) based optical stress sensing. Its performance is evaluated against more simplistic approaches, and previously demonstrated methods of optically tracking the tips of whisker sensors. The study has found the performance and sensitivity of these FBG-based sensors to be very satisfactory, with sufficient sensitivity to bending stresses to enable using Cross-Correlation (CC) and multilateration techniques (as evaluated in prior studies) to produce reliable Direction of Arrival (DoA) and velocity estimations, at a typical SNR of around 2 dB. The system has shown the capability for correction of potentially disruptive variations in temperature, allowing for effective measurement of the key hydrodynamic disturbances under study, irrespective of the local environmental conditions.

1. Introduction

With the increase in the use of unmanned or autonomous underwater vehicles, there is an emerging challenge in monitoring their environment more effectively. A challenge that demands an innovative approach to flow measurement technologies that are well suited to the challenges of the environment. In particular, when a large fleet of vehicles of this type is planned, additional demands are placed on the monitoring system, in terms of dealing with the surrounding hydrodynamic noise, both to avoid interference, and from the desire to detect quiet operators in the area. The disturbances of interest often take the form of coherent vortical structures, which both travel with the flow and are left in the wake of travelling objects such as marine life or ships. In earlier attempts to better observe different hydrodynamic disturbances, several groups have investigated the performance of simple artificial whisker sensors, either as single sensors [1,2], or as an array of sensors that react to the flow environment [3,4], often drawing useful inspiration from nature [5]. For example some approaches mimic the way that seals track objects, despite not always having precise directionality and instead resorting to "undulatory" patterns in and out of their prey's wake [6]. The previous generation of whisker sensors has regularly suffered from problems with versatility, reliability, and ultimately their sensitivity. In particular, issues of versatility and reliability have been an issue for systems that rely on visual tracking methods due to interference effects from light pollution, the presence of visual obstructions, and difficulty mounting cameras in optimal locations, all of which need to be overcome without disrupting the flow itself. The reliability concerns that are familiar with the use of electronic sensors are typically their vulnerability to any moisture ingress (via leaks or high humidity), electro-magnetic disturbances, or saltwater corrosion, which is a particular problem with electronic sensors. Fibre optic sensors (which are non-electrical and passive in operation) are well suited to overcoming these issues, taking advantage of their inert nature and resistance to water exposure, saltwater corrosion, and electro-magnetic interference.

This study has aimed to enhance the tracking of hydrodynamic disturbances, a process that can be achieved through the design and evaluation of a new class of whisker sensors, designed by combining the well-known monitoring capabilities of fibre optic sensors, with our previously demonstrated adaptations of established source localisation techniques [4,7]. The potential for using fibre optic sensors designed around FBGs, to be used as contact sensors has been explored in previous studies that used the deflection of a flexible sensor mount, to stretch the fibre and thus cause a wavelength shift [8]. Further studies

* Corresponding author.
E-mail address: raphael.glick@city.ac.uk (R. Glick).

https://doi.org/10.1016/j.optlaseng.2024.108125
Received 14 September 2023; Received in revised form 22 November 2023; Accepted 18 February 2024

have used whisker-like FBG sensors for surface mapping [9], imitating mammalian whisker use, and mimicking 'whisking' behaviour, for example as seen in rats [10,11]. The approach used therein utilises the strain sensitive nature of FBG sensors and indeed has met with some success. The displacement of the whisker tip bends the fibre sensor, and induces a predictable and measurable wavelength shift for a given displacement. Thus by carefully monitoring and then calibrating this wavelength shift, such systems have successfully been used to assessed shaped obstructions and variations in surfaces in remotely controlled environments.

Recent review studies [12,13] have highlighted a multitude of methods relying on electronic and visual tracking, including mechanisms that offer solutions to the issue of camera placement [14], as well as advances in optical sensors used for self orientation [15]. These sensors rely on the changing interference signals of a multi-beam system as the cavity lengths vary when subjected to external stimuli, allowing for pitch and roll measurement.

Building on these previous studies, in this work an optical whisker design for flow sensing and event detection has been developed, that utilises a simpler and more advantageous detection premise. Here, the strain sensitive nature of the FBG sensors can be used to detect the bending motion of the sensors. Therefore the disturbance is seen in each of the sensors' signals, as the disturbance moves across the array. The path of the hydrodynamic disturbance can therefore be tracked by observing the shift in the temporal signatures across the array of whiskers. This allows for the calculation of the velocity and direction of the disturbance by observing the Time Delay of Arrival (TDOA) in the bending-induced wavelength shifts. Such a method removes the need for detailed sensor deflection calibration, and thus avoids any issues relating to changes in fluid density or viscosity.

In this study the performance of this system is assessed, investigating the sensitivity of the sensors, including how this affects the accuracy of the subsequent flow behaviour calculations, and the relative computational cost of this approach. The study also addresses the performance impact of the sensor layout and spacing in order to optimise the hydrodynamic sensor array.

2. Materials and methods

2.1. Water tunnel arrangement

Two water flow arrangements have been used in the study, and both have used the same closed-circuit water tunnel, with a test section of 40 cm width × 50 cm depth × 120 cm length, as is illustrated in Fig. 1. Here it can be seen that the test section is transparent on all sides, allowing for visual observation of the flow behaviour, during the flow studies that are described in this paper. The model platform with the optical whisker array mounted on it was submerged in the water tunnel, along the centre-line of the test section in the mid cross-section as can be seen from the figure. A series of test arrangements was set up and in the first of these, tests were conducted in water which was initially stationary and then disturbed by vortex rings. The ring vortices had an outer diameter of 40 mm, core diameter of 28 mm, and an initial velocity of 100 cm/s. These types of disturbances could be created using a vortex cannon in a reproducible manner. A similar vortex cannon was used in previous studies to test the sensing capabilities of live seals [16], where the size and speed of the vortex ring used mimics those vortices left in the wake of prey fish in nature [17]. The vortex ring generator orifice was positioned 200-300 mm away from the front of the sensor array. This allowed for a direct comparison with the performance of a previous fibre optic sensor design from the authors (which was tested with the same equipment under similar conditions [4]).

The second arrangement used involved tests conducted in flowing water where the flow disturbances were produced by a vertically oriented cylinder with a 30 mm diameter, placed upstream of the sensors. The cylinder was used to consistently shed turbulent vortical flow features, which pass the sensor array at about 2 Hz, (per the Strouhal number of 0.21). In keeping with prior studies, the cylinder used was positioned at a series of distances in front of the array, from 10Dc (1Dc = 1 Cylinder Diameter) to 25Dc (300 - 750 mm), and the mean flow speed was varied from 10 to 25 cm/s. This approach again built on previous work from the authors, in that way allowing for a direct comparison of the performance [7].

When submerged into the flow, the bending of the slender fibres (mimicking the whisker) shows a mean bending component, which arises due to the drag of the stationary mean flow – this is a component which does not change over time. When a turbulent vortical flow feature in the flow was seen to pass the fibre, it induced an additional fluctuating part of the bending. It had been previously observed [18,4] that there are two components contributing to the vortex-induced fluctuating motion. The first was the velocity-induced drag component, which is proportional to the velocity difference between the whisker and the vortex-induced velocity field. The second was the pressure component, which arose from the influence of the pressure-field surrounding the vortex core on the whisker, and the result of which is a notable 'jerk-like' response in the motion of the whiskers [18]. This type of temporal response on the passing-by of turbulent structures can be beneficial to conditioning the original signals to achieve higher accuracy of the CC but which is not necessarily required.

2.2. Whiskers

The focus of this study has been to test the effectiveness of the design and thus the functionality of FBG-based optical whisker sensors, comparing their performance against the previously-used optical whiskers [18,7,4] which were tracked using a camera with integrated tracking software. Here the aim was to explore the benefit of the FBG-based whisker approach to monitor the outer flow field from inside the body from which the whiskers protrude. The setup used in this investigation (see Fig. 4) reflects the needs of this study, where all the whiskers protrude from a flat plate, normal to the plate, and are spaced at regular intervals. All the forces and the motion above the plate were negated by clamping the whiskers at regular intervals above the plate and fixing them to the plate where they pass through small holes drilled into the plate. Therefore it was only that part of the sensor that protruded below the plate that responds to the flow. Further and irrespective of the material used, the whisker-like fibres acted as cantilever beams, clamped at the root, free at the end, and which deflected according to the velocity-related drag force and the force due to the pressure-field induced by the vortex. Those forces changed over time when the vortices pass each sensor.

In this study, the performance of the originally-used artificial whiskers, made of 750 μm transparent polymer fibres, was taken as the 'baseline' from which the enhanced performance of the new FBG-based silica fibre sensors, designed and evaluated in this work, could be assessed. The polymer fibres were bundled together and illuminated from one end with an LED light source. The light exits at the other end, illuminating the whisker tips. The position of the whisker tip light spots was tracked by a high-speed tracking camera (as shown in Fig. 1). The polymer fibres used were 80 mm in length and 750 μm in diameter, and were arranged in a five-branch spiral array with logarithmic spacing. The design developed has been based on the key features of designs for aero-acoustic microphone arrays, which seek to minimise co-linearity for better beamforming performance [19]. Despite how closely packed the fibres appeared (as visible in Fig. 2), they were out of plane from one another, positioned roughly 0.35 whisker lengths apart. Further, due to the intentionally irregular layout of the array, at any given DoA there were only a few whiskers directly in the wake of another whisker closer than 0.6 whisker lengths, reducing the prominence of Vortex Induced Vibrations (VIV). The silica sensors used were 80 mm long and

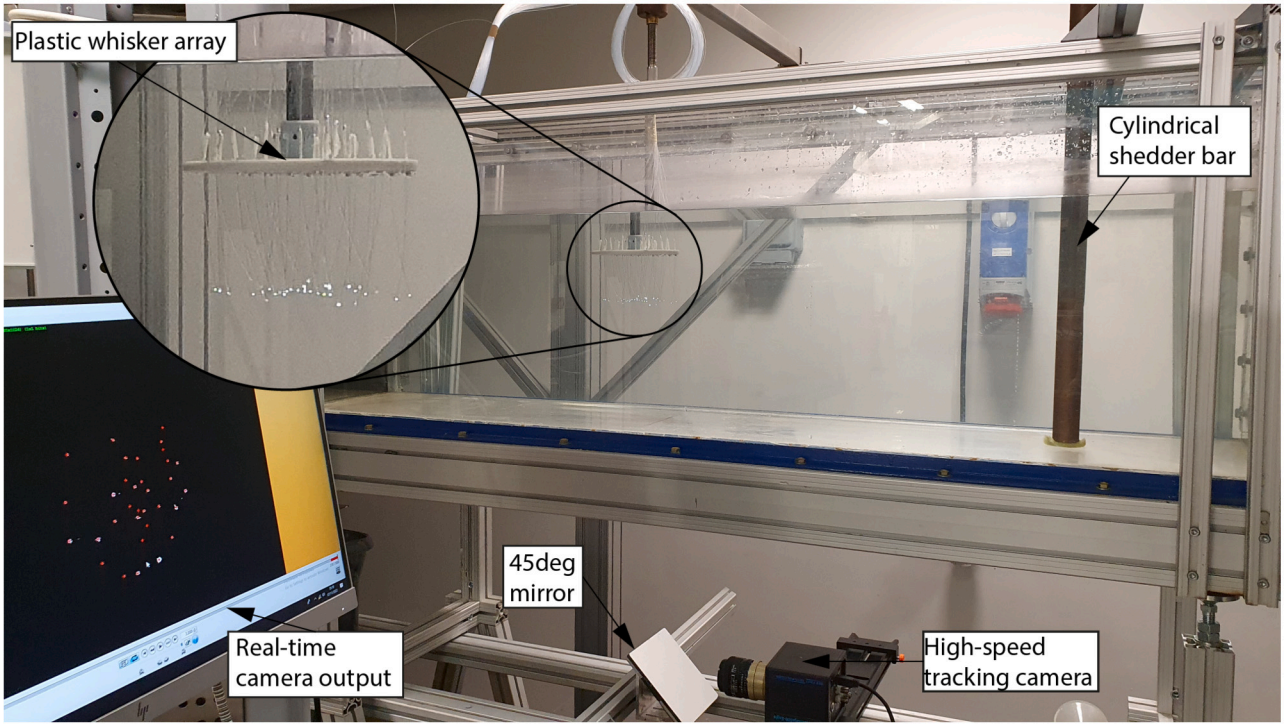

Fig. 1. Pictured is the experimental setup for flow disturbances in established flow, using a spiral array of visually tracked plastic fibre whiskers.

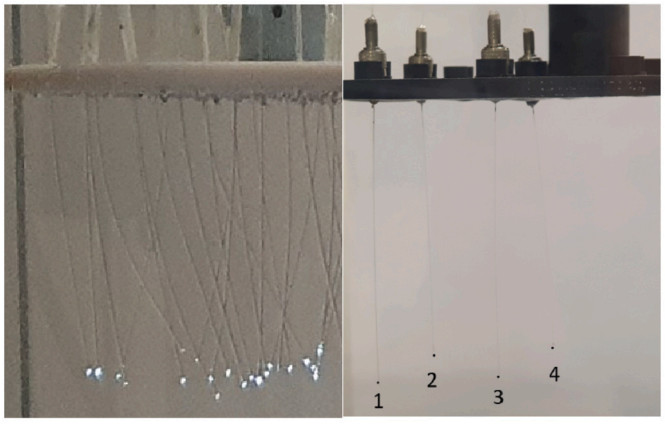

Fig. 2. Left: Plastic fibre array under disturbance from a vortex ring moving from left to right. Right: Close-up view of the glass fibre array in similar scale and position.

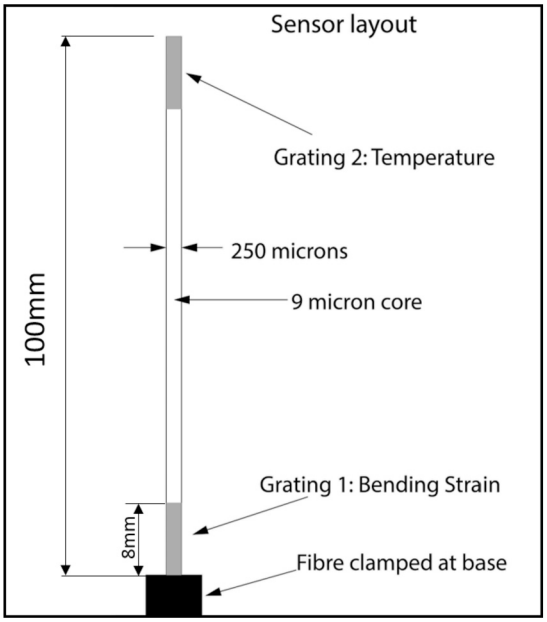

Fig. 3. Diagram of a silica optical fibre sensor. The oscillations at the sensor's eigenfrequency dominate the sensor's response to excitation in air, but are heavily damped when underwater.

were made from 250 μm diameter optical fibres, (with a 9 μm core diameter). The smaller diameter and different materials used mean that the silica fibres have lower bending resistance than the polymer fibres. On the other hand, they also have a smaller frontal area which results in lower drag force. Both effects combined resulted in a similar order of tip displacement magnitudes to the polymer fibres when observed under similar flow conditions. The key feature of the silica fibres was the set of FBGs written into them to act as strain and stress sensors. The fibres thus had an 8 mm long grating written at the root of the fibre, just beyond the clamping point, and were designed to be where the bending was concentrated, see Fig. 3.

Ordinarily, such fibres are most sensitive to axial loads and typically not very sensitive to bending. However, ensuring that the gratings used were positioned at the site of the most concentrated bending forces which maximises the sensitivity of the fibres to the bending forces. This consistently produces a measurable wavelength shift. It can be noted that temperature sensitivity is a useful secondary function of the FBG sensors (when used as temperature sensors [20]), but this means that the gratings are very sensitive to temperature fluctuations including when the measurement of any other parameter is required. To deal with this problem, an approach used in several other sensors by some of the authors [21] has been employed where a second (in this case strain relieved) grating is used to monitor any temperature fluctuations on their own. This way, the sensor system could differentiate the wavelength fluctuations due to bending alone, with this second grating placed on

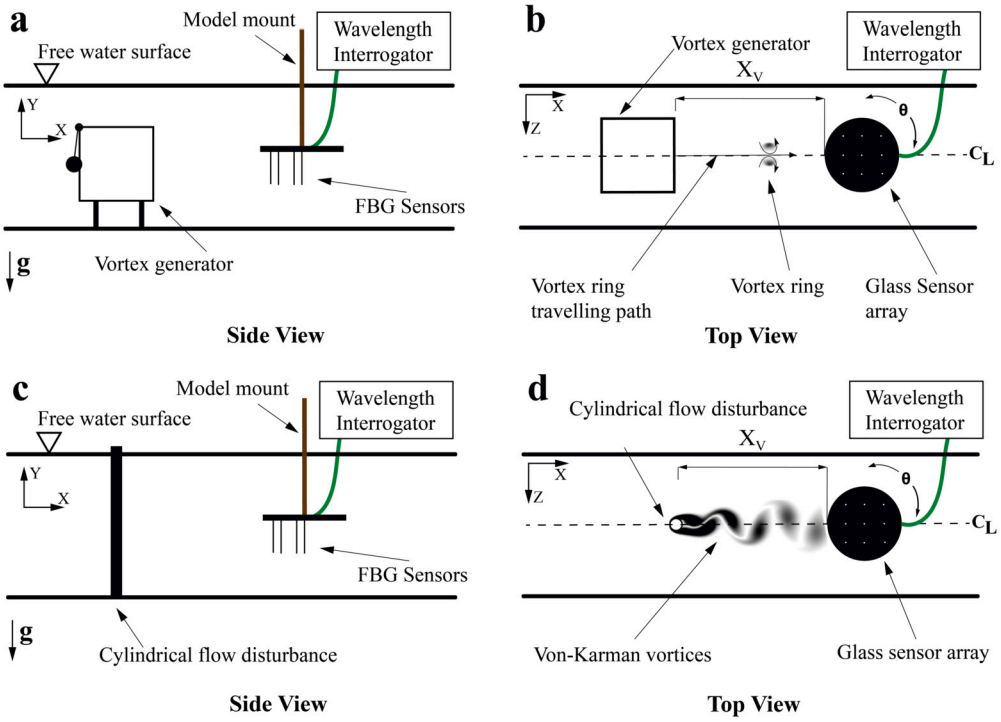

Fig. 4. (a-b) Schematic diagram of the whisker array and vortex cannon, shown here with the FBG sensors. The setup is the same for the plastic fibre arrays but with the addition of the tracking camera as pictured in Fig. 1. (c-d) Setup showing the cylinder upstream of the array. For both setups, the disturbance source remains stationary but the array is rotated about its centre.

the sensor, away from the root, and towards the tip (where the bending forces are much weaker and thus temperature is the primary measurand). This approach was used to normalise the root sensor output and thus deal with any potential interference in the measurement from any fluctuations in temperature. This was particularly important for field applications, especially in situations involving the mixing of two or more flows at different temperatures. The fibres used were glued into SMA connectors that were designed to slot into sockets built into the 3D printed plate (and visible in Fig. 2). The change in the wavelengths of the FBGs written into the fibres were monitored using a commercial FBG interrogator, (type Micron Optics sm130), which was used to track the shift in wavelength of the backscattered light from the FBG sensors, at a maximum sampling rate of 2 kHz (which was more than adequate for the work carried out). The FBG wavelength used was 1536 nm (chosen to match the spectral output of the interrogator) at 10 °C and in use showing maximum variations of less than 1 nm. The FBG sensors written into the fibres had a reflectivity of 60%, and had a bandwidth of 250 pm.

2.3. Calculation of the cross correlation & direction of arrival

The calculations conducted herein follow the same method as used for the post-processing of the tip-displacement signals from the polymer fibres in the authors' previous work [4] (See Appendix A for further information). In the case of the FBG-based whisker sensors, the bending-related frequency shift signal was processed by the Micron Optics interrogator and transformed into a digital output at 2 kHz. The method of temporal cross-correlation of the output between triplets of whiskers was used to generate the TDOA information for each whisker in the array, with the same basic Generalised Cross Correlation (GCC) algorithm [22] as described in our previous work [4]. A minor improvement to the code was implemented through the addition of a pre-CC filter that removed any undisturbed or seemingly anomalous sensor outputs and which then places less emphasis on the signals from whiskers experiencing a smaller deflection. This approach was implemented in this work, due to the much larger arrays used in the final part of the study described. It was noted that attempting to use all the sensors in the larger arrays yielded little to no improvement to the information received but had the penalty of raising the computational times very significantly. The subsequent DoA calculations undertaken also used the same method of multilateration based on acoustic source localisation techniques [23]. Herein the known spacing between the fibres at their roots was provided as an input into the calculations.

3. Results of the investigation

3.1. Sensor performance

In this study, the key information required is on the performance of the sensors and thus to verify the improvement in performance due to the new FBG-based whiskers employed. The important metrics which were used to characterize the performance of the sensors studied were as follows: sensitivity – thus the weakest signal that can be seen when a single sensor was deflected to the minimum perceivable point; the Signal-to-Noise Ratio (SNR) of the output signal; and the presence of Whisker Induced Vibrations (WIV) or Vortex Induced Vibrations (VIV) in the signal observed. The performance of the DoA algorithm used has already been assessed in a previous paper [4], (and thus this is not reproduced here), although the specific physical factors that influence that performance, including sensor length, spacing, and eigenfrequency, are briefly discussed below, for completeness. The absolute sensitivity of the sensors developed is known to depend heavily on the source of excitation. For the purpose of this study, the reasonable assumption was made that this was a vertical vortex roller, carried with the flowing water, and hitting the length of the vertically arranged whiskers evenly. For flow speeds below 5 cm/s and at cylinder distances larger than 10Dc the roller did not have enough energy to deflect the sensor sufficiently to be perceived from the output signal against the background noise. This can be regarded as the resolution limit of the FBG whiskers in the current study.

The SNR of the FBG fibres was calculated from the magnitude of the shift in the wavelength of the back-scattered light while deflected com-

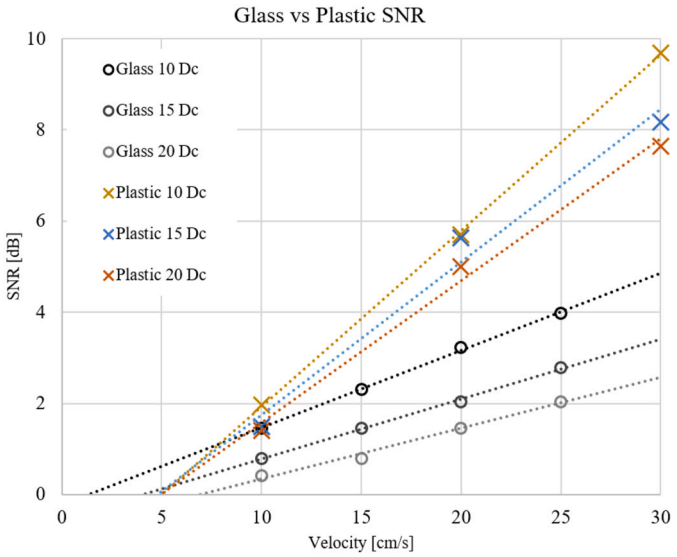

Fig. 5. The sensors were disturbed by a series of vertical vortex rollers passing by, shedding from the cylinder placed upstream of the array, and carried with the flowing water. The rollers hit the length of the sensor evenly. This signal was chosen for comparison as it is the weaker of the two signals discussed herein.

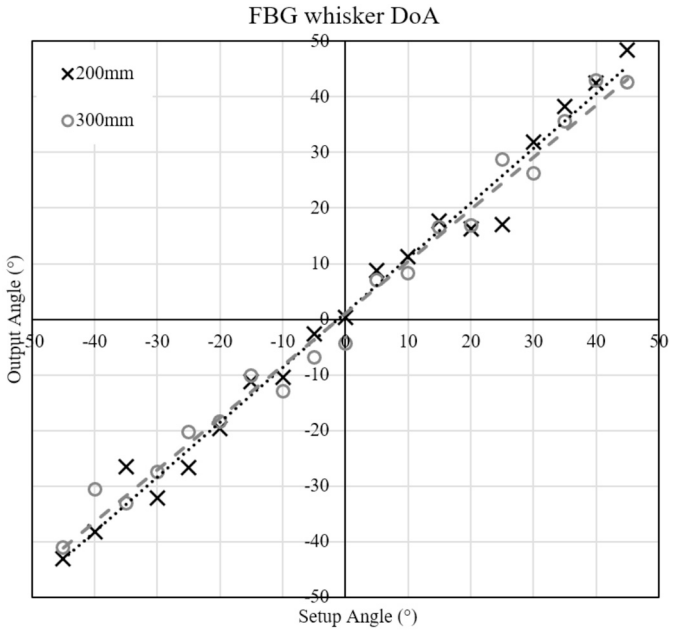

Fig. 6. Performance deteriorates slightly with distance to the source. The performance at 200-300 mm is still excellent with RMSE of 3.5° and 3.7° respectively.

pared to the maximum fluctuations in wavelength due to background noise. In comparison, the SNR of the polymer fibres was calculated from the magnitude of deflection when disturbed compared to the maximum variation in position in undisturbed flow. The overall performance of the sensors (in terms of the SNR) under the same excitation conditions can be seen in Fig. 5, with the SNR of the polymer fibres used for comparison with the performance of the FBG-based sensors (see Fig. 9 for sensor deflection characteristics). Here what can be clearly seen was the increase of SNR with increasing speed of the mean flow, which is related to the stronger forces (mean and fluctuating) imposed on the whiskers. The laboratory situation used for these tests provided the optimal conditions for evaluation of the performance of both the (FBG-based) silica and the polymer fibre sensors, where it can be seen that the polymer sensors outperform the silica sensors. However, in the 'real world', the field conditions experienced worsen the performance of the visually tracked systems (the polymer fibres) due to the presence of interference from vibrations, ambient light, and likely sub-optimal camera placement. By comparison, the SNR of the silica (FBG-based) fibres is still large enough for the calculation of the CC and DoA, where the performance is discussed below (and shown schematically in Fig. 6).

An approach to improving the SNR by filtering out some of the noise was taken by employing a wavelet domain reconstruction of the signal. This was found to offer a small improvement in the quality of the CC, but at the cost of a notable increase in computation time, making it a valuable addition for applications that are not time sensitive.

3.2. Estimation of the DOA performance

There are two metrics for the evaluation of the DOA performance of the whisker sensors developed in this work. The first is the prediction trend line, where the trend line gave an overall estimation of the accuracy of the prediction, and its gradient indicated a preference or skew towards an over or under-prediction of the direction of arrival. The distance between the intercept on the y-axis and the origin indicates any degree of angular skew present. The second metric used is the Root Mean Squared Error (RMSE) of the set of predictions, measured across the range of angles tested. In this work, repeat readings generating multiple signals could be used to improve the accuracy of the results obtained, but to do so requires repeat observations of the same source, from the same position. However, in both nature and many of the in-the-field application scenarios, the source of the disturbance would be moving, and so the occurrence of such a scenario was unlikely. Therefore, in this work, the RMSE of the sensors was calculated using single flow disturbance events. The results of such an investigation were encouraging, as overall, the prediction of the performance was very good, so long as the signal strength is sufficient to create a well-populated TDOA matrix. As the distance to the source increases, the gradient of the trend-line drops slightly, this being possibly due to the rate at which the disturbance is slowing down. The intercepts for all graphs examined were within a few degrees of the origin, indicative of a small overall skew, but giving a result which is within an acceptable range, given the typical RMSE data set of around 3.5°. The performance of the silica (FBG-based) sensors was compared to that of the polymer sensors, at distances of 200 mm and 300 mm (as can be seen in Fig. 8). It is evident that the performance of the polymer grid array was worse than that of the silica fibres, at both distances, by about 20% with the RMSE obtained being typically around 4.2°. The similarity of the goal of the most effective use of the sensors to other applications was noted, which lead to the final outcome of the study. In order to verify the impact of highly co-linear arrays on the predicted performance, a polymer fibre spiral array design (as described above) was used to capture potential performance improvements, aimed to be translated to a larger array of silica sensors. As expected, the spiral array showed a marked improvement compared to both grid arrays, with a typical RMSE of just 1.9° as shown in Fig. 7.

3.3. Computational savings

Finally, the computational savings associated with the simpler output of the new FBG-based sensor system were evaluated. When comparing the time taken to calculate the DoA it must be noted that the polymer array is larger and therefore has more sensors to track, evaluate, select from, and then on which to perform the cross correlation. Taking all this into account, the polymer fibres rely on the use of a tracking camera, the output of which requires extra steps to create the sensor tip displacement track, resulting in a like-for-like time save compared to the silica fibre, FBG-based sensors, of around 40%. This number does not account for the internal processing time of the tracking camera or the FBG interrogator (tracking the shift in wavelength of the FBG sensors), but conveniently the delay from both of these components was extremely small and could be ignored, compared to the

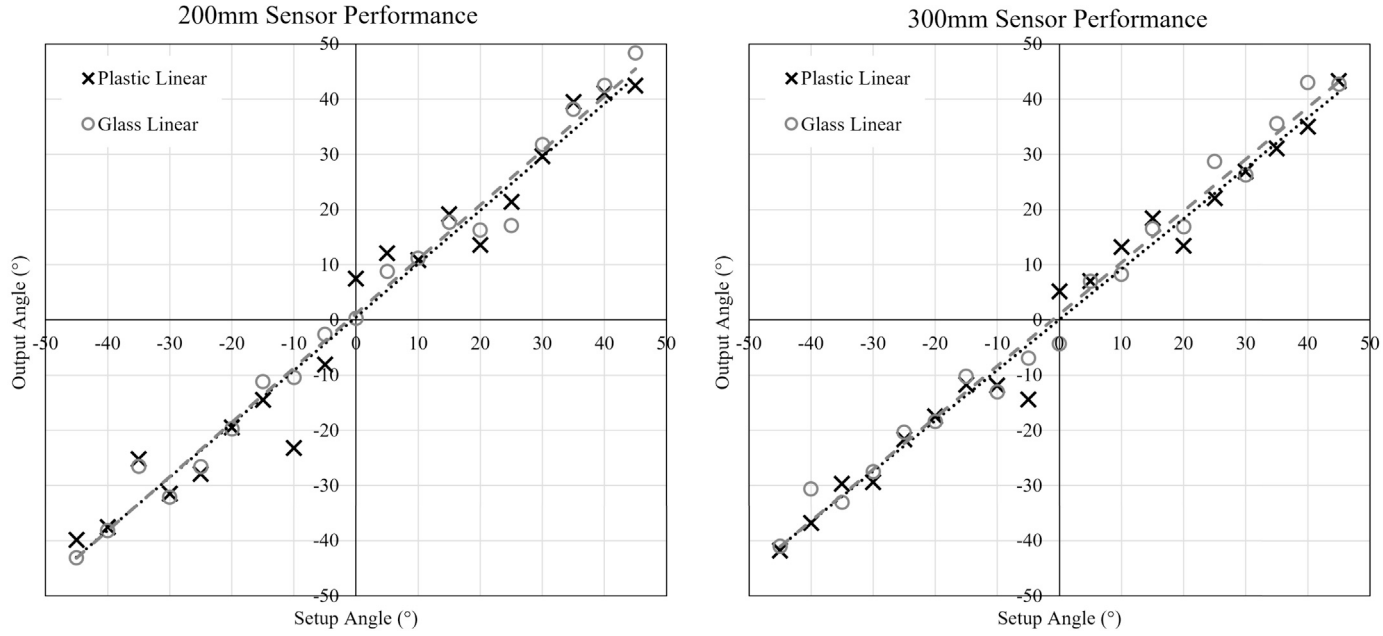

Fig. 7. Array layouts performance assessed using large numbers of visually tracked plastic sensors spaced 200 mm from the disturbance. This spiral array is inspired by similar array designs for acoustic microphone arrays, used for acoustic source localisation [19].

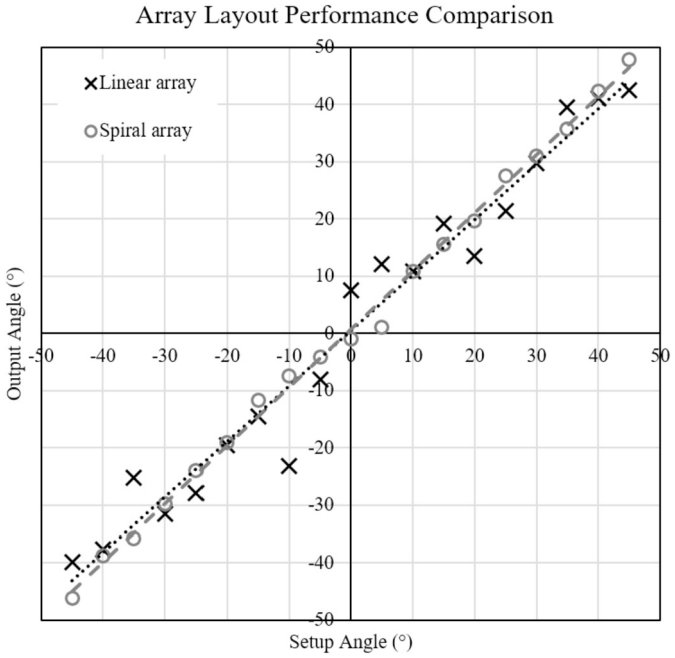

Fig. 8. Arrays spaced 200 mm from the source, with the same inter-sensor spacing.

DoA computation time. Given the value of real-time direction tracking, these improvements were significant, and with a more powerful system could potentially realize a delay of only a couple seconds which would be acceptable for most industrial applications.

4. Discussion

The data from the investigation has shown that the square arrangement of the four FBG-based sensors in the silica fibre offered a real performance improvement over the larger, grid array of polymer sensors, even though the individual SNR figures for these sensors were somewhat poorer than those of the sensors in the polymer fibre. This result was obtained for the investigation carried out under laboratory conditions, but it can be noted that the FBG-based sensors will perform better in the field, due to the different scaling factor of the size of the disturbance (the vortex diameter), relative to the spacing between the fibres in the two different arrays. When evaluating the silica sensors, the array and disturbance source were carefully aligned such that all four sensors would fully experience the effect of the disturbance each time. For the larger 2D array, the significant co-linearity of the array may have made several of the disturbed whiskers redundant. A potential way to overcome this effect is to use an array with non-linear spacing such as in the spiral arrangement, also commonly employed in audio-cameras when using beamforming reconstruction algorithms for source localization. As can be seen from Fig. 6, the further the array is positioned from the disturbance, the shallower the gradient of the trend line, i.e. the tendency is then to a potential underestimation of the angle to the disturbance. This effect is expected as the vorticity field dissipates with the distance travelled from the source and therefore the energy of the disturbance exciting the sensors decreases and approaches at some distance the noise level experienced for an individual whisker.

The SNR of the FBG-based sensors written into the silica fibres due to the imposed bending stress from the flow-induced forces overall is at a low level, indicating that this alone cannot be a sufficient indicator of flow speed or direction. However, as the correlation principle of temporal differences in the response of fibres in the array is being used, the convection velocity at which the disturbance travels and the direction from where it hits the array can be calculated. Therefore, under the conditions presented herein, and using the methods as described above to process the signals, the data were sufficient to track the source's disturbances. Under less favourable conditions, or when facing weaker stimuli, a higher SNR would likely be preferable. In order to track a single source when multiple sources are present, i.e. in an environment with higher background noise, a greater sensitivity would be preferable. To achieve this, further work could be done on mechanical changes to the whisker size and strength to optimize these to enable adjusting the minimum required force on the sensor to be greater or smaller as needed.

In this research, fibres of a core diameter of 4 μm were tried first, but these did not produce sufficient wavelength shift under deflection. Fortunately, alternatives are available and so FBGs were written into

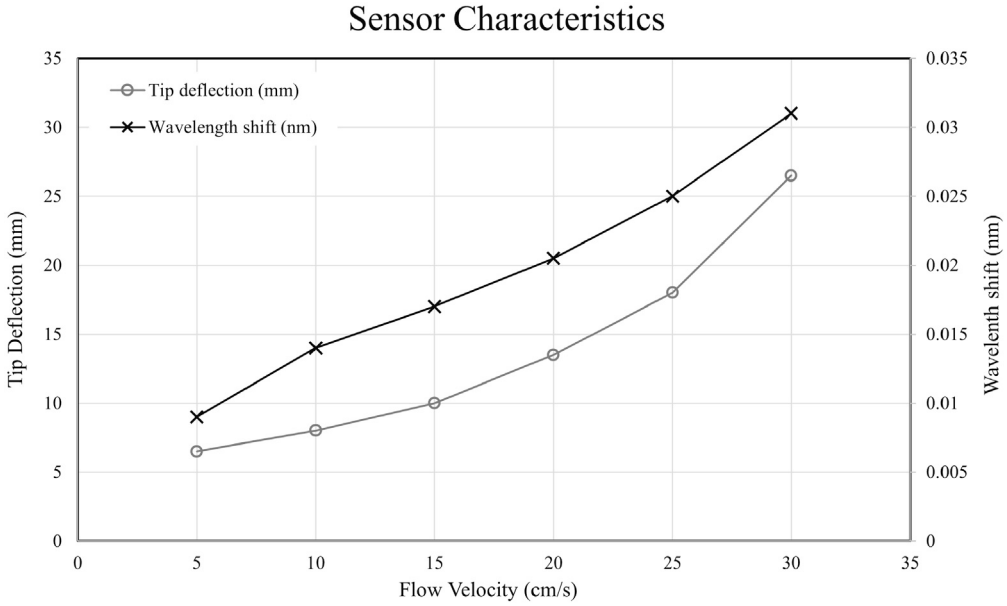

Fig. 9. Sensor performance in turbulent flow. The array of sensors can function provided the magnitude of the wavelength shift is sufficient to allow for reliable inter-sensor CC, (around 0.012 nm given present noise levels of ±0.006 nm).

larger core (9 μm) fibres, and these were found to give sufficient compression/expansion of the FBG and resultant change in wavelength. Contrary to conventional usage, under bending stress, a wider core results in a larger wavelength shift. The wider core results in the outer section of the fibre core being subject to greater strain due to the cross-sectional load concentration of a beam under bending stress, resulting in a larger wavelength shift.

There is further scope for enhancing the sensor performance by making changes to the whisker profile and cross-section as this could alter the drag force at a given flow velocity, thus changing the threshold flow speed at which the whisker starts moving (and thus this can be detected). Further enhancement of the system could be achieved by stiffening the fibres (apart from at the root), as this could offer potential improvements to the SNR by capturing more of the bending motion occurring at the root of the fibre (where the FBG is positioned), rather than allowing the typical bending profile of a uniform beam where some of the bending would occur along the length of the beam.

The main limitation of such an approach is to avoid the sensors becoming overly sensitive to shocks and knocks (and thus require more protection with additional coating). A downside of such an approach is that the stiffness created in the fibre may then counteract any additional sensitivity gains. The process used to re-apply the polymer coating to the engraved optical fibres could have also contributed to a decrease in the sensitivity of the whiskers (as the writing of the FBGs in the fibre requires the removal of the primary coating, which is then reapplied to protect the fibre). The re-coated sensor's polymer coating was slightly thicker than the original coating (by about 20-30 μm). This thicker coating was located inevitably at the position of written FBG, thus with a potential impact on sensitivity. A further minor issue is that the wider re-coated fibre root did not fit exactly into the standard-sized fibre SMA connectors which were used to secure the fibre and therefore a larger connector had to be used, with the fibres glued in place. Unfortunately, this larger orifice still did not clamp the fibre perfectly, which could have let the fibre deflect a little behind the clamping point, thereby reducing the bending at the grating, and therefore the sensitivity of the sensor.

The above points to several of the potential enhancements to the system that could be implemented in future work, building on the success of the results obtained from this investigation.

5. Conclusions

The work done has been innovative in its approach, using FBGs written into silica fibre, to create a very effective means of tracking hydrodynamic disturbances with fibre optic whiskers. The study carried out has shown that such an array of FBG sensors can produce very good estimations of the velocity and DoA of flow disturbances which pass the sensors. An important feature of the design is that a small number of fibres are used, offering high-quality, reliable and rapid measurement with an array consisting of only 4 sensors (in a grid arrangement). The results obtained have demonstrated the precision of the measurements made, based on the principle described, showing that it would be possible to build an effective array of this type of FBG-based whisker sensors mounted on unmanned underwater vehicles to track passing objects. As demonstrated with a larger array, it is easy to increase the number of sensors (by simply adding more FBGs written at different wavelengths into the fibres, as the Micron Optics interrogator used has considerable scope for detecting over a wider bandwidth), offering an improved layout which can further improve the DoA estimates. Thus in further work, scaling up the array is a key target.

In this research, methods to increase the potential precision were tested and show some promising trends. Furthermore, machine learning is a valuable tool that could be brought to bear on this problem and thus could potentially improve signal tracing, allowing for better performance at lower SNR, or offering valuable SNR enhancement. Supporting this, Elshalakani et al. [24] have demonstrated that machine learning can make good predictions in whisker systems, based on RMS values of the bending magnitude. There is therefore good reason to suggest that it could do the same with time-domain based DoA estimations helping with filtering, or processing the signal at various stages of operation. Thus there is considerable scope for enhancing the performance of the system in the ongoing research into this interesting phenomenon.

CRediT authorship contribution statement

Raphael Glick: Conceptualization, Data curation, Formal analysis, Investigation, Methodology, Writing – original draft, Writing – review & editing. **Christoph Brücker:** Conceptualization, Funding acquisition, Project administration, Resources, Supervision, Writing – original draft, Writing – review & editing. **Matthias Fabian:** Conceptualization,

Methodology, Resources, Writing – review & editing. **Kenneth T.V. Grattan:** Conceptualization, Project administration, Supervision, Writing – review & editing.

Declaration of competing interest

The authors declare the following financial interests/personal relationships which may be considered as potential competing interests: Christoph Bruecker reports financial support was jointly provided by BAE Systems and the Royal Academy of Engineering, Research Chair No. RCSRF1617\4\11.

Data availability

Data will be made available on request.

Appendix A. Direction of arrival calculations

The following calculations are largely reproduced from the authors' previous work [4], and included here for the readers' convenience:

The Direction of Arrival is defined as the angle between the oncoming vortex ring and the anteroposterior axis of the model, in the horizontal plane. The bow-wake effect of the travelling vortex ring is causing the initial deflection of the whiskers and is approximated across small distances as a signal propagating with a planar wavefront.

The inputs to the multilateration function are the arrays of time delays between every pair of whiskers, and the X and Y position of each whisker tip while the whisker is at rest. The time delays are calculated via a Generalised Cross Correlation function [22], as a function of the whiskers displacement.

The calculation relies on the basic principle of TDOA multilateration. It differs from other conventional use cases in that both the time of the signal's emission and the speed of the signal are unknown. To account for this, triplets of sensors are used instead of pairs that are typically used when the speed of the signal, or the signal emission time is known. This allows for the calculation of the DoA by comparing the ratio of the TDOA with the ratio of the distance between the sensors, a comparison that is independent of the signal's velocity or time of emission.

Assuming that the direction and velocity of the signal remain constant while travelling over the triplet of sensors, then the time difference between the excitation of the three whiskers of known position should produce the angle and velocity of the signal as follows:

$$\frac{\Delta T_{AB}}{\Delta T_{BC}} = \frac{L_{AB}(\gamma)}{L_{BC}(\gamma)} \tag{1}$$

where 'ΔT' is the time difference between the whiskers A and B, and 'L' is the distance between points A and B in the direction of travel, (γ).

$$L_{AB}(\gamma) = cos(\Theta_{AB})\sqrt{(x_B - x_A)^2 + (z_B - z_A)^2} \tag{2}$$

The coordinates 'x' and 'z' represent the pixel positions of whisker tips A and B, and Θ_{AB} is the angle between $L_{AB}(\gamma)$ and the line AB:

$$\Theta_{AB} = 180 - \gamma - \alpha_{AB} \tag{3}$$

where 'α_{AB}' is the angle between the distance vector $\vec{AB}$ and the z-axis, and 'γ' is the angle of the propagating signal front.

To find the solution, an algorithm is applied that scans all possible values of γ, from -90 to 90 degrees in 0.002-degree increments, recording the range of values of γ that satisfy equation (1) to four significant figures. The size of the range of resulting values provides an estimate of the uncertainty in the angle output of that whisker triplet and is mostly dominated by the size of γ, as small angles result in small time delays between whiskers in the triplet, which are therefore more sensitive to random error. This is repeated for all viable triplets of whiskers (with low co-linearity and sufficient deflection), and the result is taken from the displacement-weighted average of the γ outputs:

$$\bar{\gamma} = \frac{\sum_{n=1}^{m}(\gamma_m * \frac{MinD}{\bar{D}})}{m} \tag{4}$$

where 'MinD' is the minimum displacement of any whisker in the triplet, and '$\bar{D}$' is the average whisker displacement across all measurements. The travel velocity of the signal is therefore simply calculated as:

$$\hat{V}_s = \frac{\sum_{n=2}^{p} \frac{L_{1,n}(\bar{\gamma})}{\Delta T_{1,n}}}{p-1} \tag{5}$$

where $L_{1,n}(\bar{\gamma})$ is the length between points 1 and n, at the calculated $\bar{\gamma}$, and $\Delta T_{1,n}$ is the corresponding time delay.

Error in the calculated travel velocity of the vortex ring due to vertical variation in vortex exit angles (maximum measured angle variations of ±2.7°) is calculated as follows:

$$\%Error = \frac{\hat{V}_s - \hat{V}_s * Cos(2.7°)}{\hat{V}_s * Cos(2.7°)} * 100 \tag{6}$$

The lowest recorded vortex ring velocities were roughly 1 m/s, leading to a maximum velocity error of 0.11%.

References

[1] Zhang X, et al. Harbor seal whisker inspired self-powered piezoelectric sensor for detecting the underwater flow angle of attack and velocity. IMEKO 2021;172:180866.
[2] Liu G, Jiang Y, Wu P, Ma Z, Chen H, Zhang D. Artificial whisker sensor with undulated morphology and self-spread piezoresistors for diverse flow analyses. Soft Robot 2022;10(1).
[3] Xu P, et al. A triboelectric-based artificial whisker for reactive obstacle avoidance and local mapping. Research 2021;2021.
[4] Glick R, Muthuramalingam M, Brücker C. Sea lions could use multilateration localization for object tracking as tested with bio-inspired whisker arrays. Sci Rep 2022;12:2045–322.
[5] Adachi T, et al. Whiskers as hydrodynamic prey sensors in foraging seals. Proc Natl Acad Sci 2022;119:e2119502119.
[6] Schulte-Pelkum N, Wieskotten S, Hanke W, et al. Tracking of biogenic hydrodynamic trails in harbour seals (phoca vitulina). J Exp Biol 2007;210:781–7.
[7] Glick R, Muthuramalingam M, Brücker C. Fluid-structure interaction of flexible whisker-type beams and its implications for flow sensing by pair-wise correlation. Fluids 2021;6(3):102.
[8] Heo J, Chung J, Lee J. Tactile sensor arrays using fiber Bragg grating sensors. Sens Actuators A, Phys 2006;126(2):312–27.
[9] Zhao C, Jiang Q, Li Y. A novel biomimetic whisker technology based on fiber Bragg grating and its application. Meas Sci Technol 2017;28:095104.
[10] Jadhav S, Feldman D. Texture coding in the whisker system. Curr Opin Neurol 2010;20:313–8.
[11] Morita T, Kang H, Wolfe J, Jadhav S, Feldman D. Psychometric curve and behavioral strategies for whisker-based texture discrimination in rats. PLoS ONE 2011;6(6):e20437.
[12] Wang S, et al. Potential applications of whisker sensors in marine science and engineering: a review. J Mar Sci Eng 2023;11:2108.
[13] Hollenbeck A, Grandhi R, Hansen J, Pankonien A. Bioinspired artificial hair sensors for flight-by-feel of unmanned aerial vehicles: a review. AIAA J 2023:1–26.
[14] Kent TA, Kim S, Kornilowicz G, Yuan W, Hartmann MJZ, Bergbreiter S. Whisksight: a reconfigurable, vision-based, optical whisker sensing array for simultaneous contact, airflow, and inertia stimulus detection. IEEE Robot Autom Lett 2021;6:3357–64.
[15] Wang J, Yang X, Wang A, Jiang H, Bai L, Meng H, et al. Bio-inspired fiber attitude sensor for direction-distinguishable pitching and rolling sensing. J Lightwave Technol 2023;41:6844–51.
[16] Krüger Y, Hanke W, Miersch L, Dehnhardt G. Detection and direction discrimination of single vortex rings by harbour seals (phoca vitulina). J Exp Biol 2018:221.
[17] Hanke W, Bleckmann H. The hydrodynamic trails of lepomis gibbosus (centrarchidae), colomesus psittacus (tetraodontidae) and thysochromis ansorgii (cichlidae) investigated with scanning particle image velocimetry. J Exp Biol 2004;207:1585–96.
[18] Muthuramalingam M, Brücker C. Seal and sea lion whiskers detect slips of vortices similar as rats sense textures. Sci Rep 2019;9:12808.
[19] Arcondoulis E, Doolan C, Brooks L, Zander A. A modification to logarithmic spiral beamforming arrays for aeroacoustic applications. In: 17th AIAA/CEAS aeroacoustics conference (32nd AIAA aeroacoustics conference); 2011. p. 1–12.
[20] Pal S, et al. Strain-independent temperature measurement using a type-I and type-IIA optical fiber Bragg grating combination. Rev Sci Instrum 2004;75(5):1327–31.
[21] Rente B, et al. Extended study of fiber optic-based humidity sensing system performance for sewer network condition monitoring. IEEE Sens J 2021;21(6):7665–71.
[22] Knapp CH. The generalized correlation method for estimation of time delay. IEEE Trans Audio Speech Lang Process 1976;24(4):320–7.

[23] Ollivier B, Pepperell A, Halstead Z, Hioka Y. Noise robust bird call localisation using the generalised cross-correlation with phase transform in the wavelet domain. J Acoust Soc Am 2019;146:4650–63.

[24] Elshalakani M, Muthuramalingam M, Bruecker C. A deep-learning model for underwater position sensing of a wake's source using artificial seal whiskers. Sensors 2020;20:3522.